Proc. Natl. Acad. Sci. USA
Vol. 76, No. 3, pp. 1109–1113, March 1979
Biochemistry

Rapid helix–coil transitions in the S-2 region of myosin

(muscle/temperature jump/kinetics/crossbridge interaction)

TIAN YOW TSONG*, TRUDY KARR†, AND WILLIAM F. HARRINGTON†

*Department of Physiological Chemistry and †Department of Biology, The Johns Hopkins University, Baltimore, Maryland 21218

Contributed by William F. Harrington, December 8, 1978

ABSTRACT **Temperature-jump studies on the long S-2 fragment (100,000 daltons) isolated from myosin show that this structure can undergo α-helix–random coil transitions in a time range approximating the cycle time of a crossbridge. Two relaxation times are observed after temperature jumps of 5°C over the range 35–55°C, one in the submillisecond (τ_f) and the other in the millisecond (τ_s) time ranges. Both processes exhibit maxima near the midpoint of the helix–coil transition (t_m = 45 ± 2°C) as determined by optical rotation melt experiments. Similar results were observed for the low temperature transition (t_m = 45°C) of the myosin rod. Viscosity studies reveal that the S-2 particle has significant flexibility at physiological temperature. Results are considered in terms of the Huxley–Simmons and helix–coil transition models for force generation in muscle.**

The subfragment 2 (S-2) region of the myosin molecule plays a major role in most current theories of muscle contraction. In the model of H. E. Huxley (1) for contraction, this segment, which forms the coiled-coil α-helical tail of heavy meromyosin, swings away from the thick filament surface during each contractile cycle of a crossbridge, thus allowing the myosin heads (S-1 subunits) to attach to neighboring thin filaments with the same stereospecific orientation over a wide range of interfilament spacing. S-2 is considered to be a rigid, inextensible rod which is fastened to the thick filament backbone by a hinge at the junction of light meromyosin (LMM) and heavy meromyosin (HMM) and is joined to the myosin head by a second hinge—the S-1/S-2 linkage. This arrangement provides the freedom required to accommodate the variable interfilament spacing as the sarcomere shortens. After attachment of the S-1 subunit to the thin filament, it rotates relative to this structure, generating a relative sliding force between the thick and thin filaments. During each cycle of a crossbridge, ATP is hydrolyzed. In the A. F. Huxley–Simmons model (2–4), S-2 serves as an elastic element which, by spring-like extension, acts to exert a part of the tensile force developed when a crossbridge interacts with the thin filament. The force-generating event is again considered to be rotation of the myosin head on the thin filament with the S-2 elastic element stretching instantaneously as the S-1 subunit alters its angle of attachment through a series of stable positions with progressively lower potential energy.

In the Harrington model (5) for contraction, the force-generating event is considered to be an α helix–random coil transition within the S-2 element during each cycle of a crossbridge. In this model the myosin head remains fixed in orientation during its transient attachment to the thin filament and the melting of part of the double α helix near the LMM–HMM junction is effected by the ATP cleavage reaction occurring on a neighboring myosin head.

Our crosslinking studies of synthetic myosin thick filaments and glycerinated rabbit muscle fibers in rigor indicate that the myosin heads, and therefore the S-2 elements, lie close to the filament surface at neutral pH (6–8). The long S-2 fragment (M_r 100,000), prepared by chymotryptic digestion of HMM (9), shows a significant tendency to self-associate, and we have proposed (10) that this association results from the presence of a sticky region near the LMM–HMM junction which serves to fasten the S-2 segment of myosin to the thick filament surface. The S-2 fragment shows a broad, monophasic thermal melting profile over the range 0–75°C with about 25% of the structure in the random-coil state at physiological temperature and ionic strength. Thus the physicochemical properties of this region of the myosin molecule, if it were to move out transiently from the stabilizing environment of the thick filament surface during each crossbridge cycle, would seem to be particularly well suited for force generation by the helix–coil transition process. In this paper we provide evidence that the double α-helical structure of S-2 can undergo helix–coil transitions on a time scale approximating the cycle time of a crossbridge.

MATERIALS AND METHODS

Preparation of Myosin Fragments. The high-molecular-weight S-2 (M_r 100,000) was prepared from chymotryptic HMM (11) by the procedure described by Sutoh *et al.* (10). Myosin rod was prepared by the procedure of Harrington and Burke (12). Rabbit psoas was used for all preparations.

Temperature-Jump Studies. The temperature-jump experiments were performed with an Eigen–de Maeyer temperature-jump apparatus (13) using a cell with optical pathlength of 0.7 mm. The signals obtained in the temperature-jump experiments are equivalent to 0.15 *A* per volt, with which the absorbance change per degree jump can be estimated. The initial temperature of the sample solution was recorded by a calibrated thermal probe in contact with the upper electrode of the cell, and the magnitude of the temperature jump was calculated according to the relation $\Delta t = CV^2/8.36\, C_P \rho v$, in which CV, C_P, ρ, and v denote, respectively, the capacitance and voltage of the charged capacitor, heat capacity, density, and effective volume of the solution. C_P and ρ were taken as unity. The effective volume, v, was determined to be 0.47 ml (14). In most measurements we used a 5°C jump. The relaxation time was then recorded at the final temperature, and the signal change per degree was recorded as the mean of the initial and the final temperatures. We used a McPherson 707K spectrophotometer for the optical density measurements of the equilibrium melting curves and a heating rate of 18°C/hr.

Optical Rotation Measurements. A Cary 60 spectropolarimeter was used for optical rotation measurements of the melting curve of the S-2 fragment as described (15). Temperature was maintained for 20 min at each step (2–5°C) over the range 4–80°C. We assumed 100% α-helical structure for S-2 at 0°C ($[m']_{233} = -16{,}000$) and 0% helix at 80°C ($[m']_{233}$ =

The publication costs of this article were defrayed in part by page charge payment. This article must therefore be hereby marked "*advertisement*" in accordance with 18 U. S. C. §1734 solely to indicate this fact.

Abbreviations: S-2, subfragment 2; S-1, subfragment 1; HMM, heavy meromyosin; LMM, light meromyosin.

−4000) in calculating the fractional helical content of S-2 at intermediate temperatures.

Viscosity Measurements. Viscosity measurements were made on the S-2 fragment in 0.1 M NaCl/20 mM phosphate, pH 7.0, with an Ostwald-type viscometer with an average rate of shear ≈150 sec^{-1}. Solvent outflow time was 130 ± 0.2 sec at 10°C.

RESULTS

Optical Rotation Changes Accompanying Melting of S-2. Fig. 1 shows a plot of the fraction of α-helical structure, f_h, of the S-2 particle (M_r 100,000) as a function of temperature derived from optical rotation melt curves (see *Inset*) at various protein concentrations. At physiological temperature, approximately 25% of the S-2 structure exists in the unfolded, coiled state. We observed no systematic differences in the midpoint of the transition (t_m = 45 ± 2°C) or in the plots of f_h against temperature of this system over the concentration range (0.034–18.3 mg/ml) investigated in the present study. The gradual melting of the two-stranded helical structure of S-2 is accompanied by a corresponding decrease in reduced viscosity (Fig. 1), consistent with an increase in the flexibility of the particle with increasing temperature.

When the temperature of S-2 solutions (concentration ≈0.035 mg/ml) was shifted abruptly in the polarimeter cell from 7 to 45°C to open the helical conformation or from 75 to 41°C to reform the α helix from the random coil state, >95% of the mean residue rotation ($[m']_{233}$) of the equilibrium melt curve was recovered within the time of temperature equilibration (<1 min). Thus, it seems clear that the opening and closing rates of the S-2 structure occur on a time scale too fast for measurement in the polarimeter cell and we therefore used the temperature-jump technique to investigate the kinetics of these transitions.

UV Absorbance Changes Accompanying Melting of S-2. Temperature-jump experiments on the S-2 fragment have been carried out at different wavelengths of incident light over the spectral range 300–220 nm and a difference spectrum was obtained. The difference spectrum has a minimum at 236 nm, a crossover at 247 nm, and a maximum at 250 nm. The total density change per degree temperature jump (for a jump from 40° to 45°C) is about -3.6×10^{-3}/mg of protein at 236 nm and 0.35×10^{-3}/mg of protein at 250 nm. No absorbance difference was observed in the 280- to 290-nm spectral region of tyrosine and tryptophan. At least three types of chromophoric groups, aromatic amino acids, amide backbone, and cysteine, are known to have absorbance bands around 235 nm. Since the absorbance change of the aromatic amino acids at the 290-nm region is expected to be comparable in magnitude to that at 235 nm upon exposure of these chromophores and since this was not the case in our experiment, the optical signal observed at 235 nm probably results from a change in the environment of cysteine residues or amide backbone in the protein molecule during the helix–coil transition. The S-2 region of myosin contains about six cysteine residues (16).

Fig. 2 gives oscillograph records of the change in optical absorbance at 235 nm after a 10°C temperature jump (35° to 45°C) of an S-2 solution in 0.1 M NaCl, at pH 7.0. Two relaxation times, one in the submillisecond (τ_f) and the other in the 5-msec (τ_s) time range, have been resolved. Although both relaxation times were independent of the S-2 concentration in the range 0.5–8 mg/ml, the magnitude of the signals was roughly linear with protein concentration only when it was below 3 mg/ml. Earlier studies of Sutoh *et al.* (10) showed that S-2 exists practically all in the monomer form below 3 mg/ml, and our temperature-jump experiments have therefore been limited to this range of concentration.

The relaxation times of helix–coil transitions in synthetic homopolymers occur in 10^{-7}- to 10^{-8}-sec time ranges (17). The rapid phase of the folding–unfolding transition of globular proteins takes place in the 50-msec time range (18). Thus, the

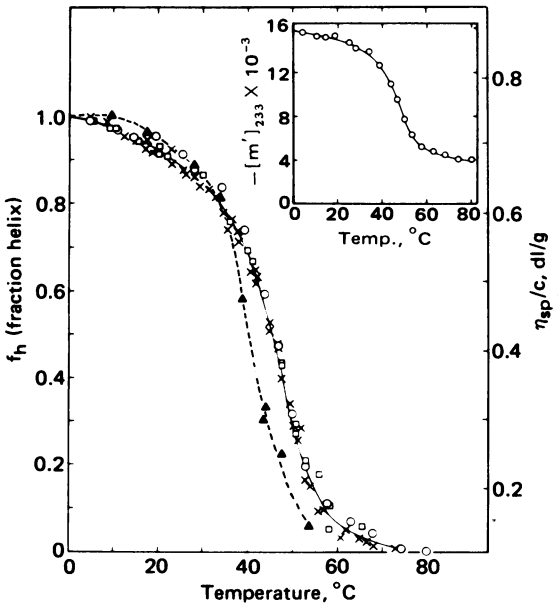

FIG. 1. Fraction of α-helix (f_h) against temperature of S-2. S-2: 18.3 mg/ml (□), 3.9 mg/ml (○), 0.034 mg/ml (×). Derived from optical rotation melting curve (*Inset*, 3.9 mg/ml). ▲, Reduced viscosity of long S-2 against temperature; protein concentrations, 2.9 mg/ml. Solvent is 0.1 M NaCl/20 mM phosphate, pH 7.0.

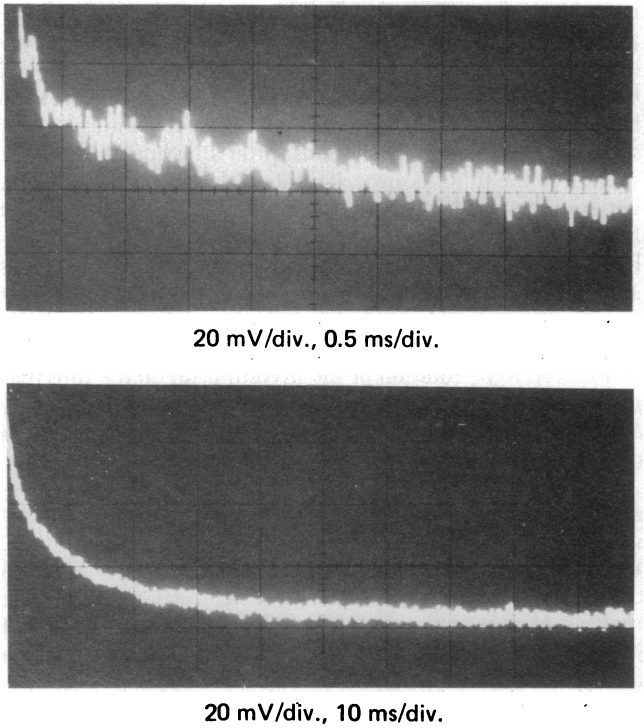

FIG. 2. Oscilloscope records of a rapid temperature jump of S-2. An S-2 solution of 0.5 mg/ml in 0.1 M NaCl/20 mM phosphate, pH 7.0, was subjected to a temperature jump from 35° to 45°C. Oscillograph records a fast relaxation (τ_f = 0.7 msec) (*Upper*) and a slower relaxation (τ_s = 12 msec) (*Lower*). The signal was measured at 235 nm, 1 V = 0.15 absorbance change.

helix–coil transitions in S-2 seem to correlate better with the rapid phase of a protein-unfolding reaction. [Note that there is no proline in the S-2 segment (16)]. The reduced rate for the helix–coil transition in S-2 may be explained by the fact that this region of myosin is a double-stranded helix with a heterogeneous amino-acid composition. Thus, the melting transitions involve molecular interactions resembling more that of proteins than that of peptide homopolymers. As mentioned, since the two relaxations are independent of the protein concentration, they do not appear to be related to a strand separation of the peptide chains in these particles. Separation of the double helix presumably does not occur under these experimental conditions.

A plot of the derivative $\Delta[m']_{233}$/deg of the S-2 melting profile obtained from the plot of optical rotation against temperature of S-2 is shown in Fig. 3*A*. This plot shows a broad, monophasic transition with maximum near 43°C. Thermal melting studies at different protein concentrations over the range 0.0035–1.3% gave similar behavior with maximum varying between 43 and 47°C. No significant differences in melting behavior of the S-2 fragment were detected after an additional purification step on Sephadex G-200.

The signal measured in the oscillograph records of Fig. 2 also show a maximum for both τ_f and τ_s near 43°C (Fig. 3*B*) when ΔA_{233}/deg is plotted against the mean temperature in the *t*-jump.

Equilibrium measurements of the helix–coil thermal transitions, monitored by absorbance changes at 235 nm, are given for S-2 in Fig. 3*C*. A gradual increase in absorbance well below the t_m of the helix–coil transition was observed. This change is too fast to be resolved by our temperature-jump apparatus (faster than a few μsec). The source of this optical change is not yet clear, but a similar increase in absorbance for ribonuclease A has been observed (unpublished results) at the same wavelength before the known unfolding transition. The transition temperature of S-2 in Fig. 3*C* agrees with that obtained in the temperature-jump experiment—i.e., 43°C. The transition in absorbance appears to be sharper than the transition in optical rotation. We note, however, that the dramatic increase in absorbance at temperatures much below the melting point could deceptively sharpen the transition curves by overlapping with the drop in absorbance of the helix–coil transition. In fact, the combined temperature-jump signals of Fig. 3*B* can be integrated, and the curve obtained shows a much broader transition, consistent with the broad melt curve of $[m']_{233}$ against temperature of Fig. 1. The integrated curve has a ΔA of about 0.04/mg of S-2 protein per ml in the range of 30°–55°C. This value is slightly lower than that estimated from the transition curve of S-2 in Fig. 3*C*. Approximately 10–30% of the equilibrium optical change has escaped our kinetic measurement, and the absorption change undetected in temperature jump could occur either in a much faster (<2 μsec) or in a much slower (>0.5 sec) time scale than the time range studied here.

Dependence of Relaxation Time on Temperature. Both relaxation times of S-2 exhibit maxima near the t_m of the helix–coil transition (Fig. 4). This type of behavior has been seen in the helix–coil transitions of homopolypeptides (17) and in the folding–unfolding transition of small globular proteins (18).

The biphasic kinetics could mean two things: either the reaction involves three states (i.e., one intermediate state) or the reaction is a cooperative transition of two broadly distributed states (19). If we assume for simplicity that the reaction is of the two-state nature and t_s reflects the rate-limiting step, then at higher temperature τ_s is equivalent to a time constant for the melting of the helix and at low temperatures it is equivalent to a time constant for the formation of the helix. Thus, both the opening and closing reactions of the helical structure occur in the 5-msec time range.

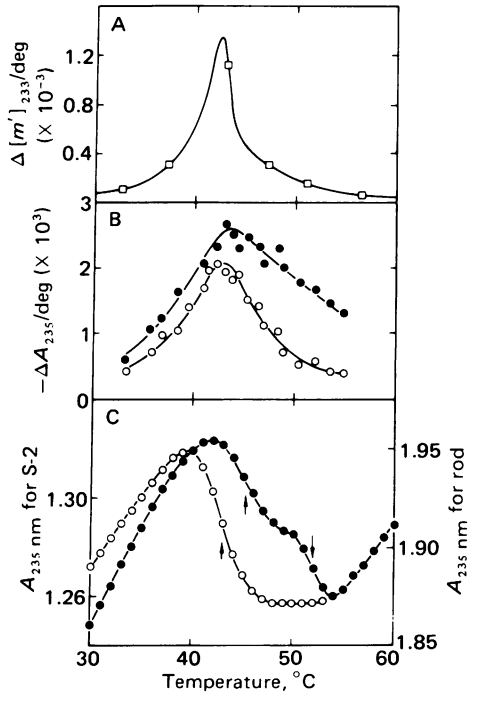

FIG. 3. Optical signals associated with the helix–coil transition of S-2 and myosin rod. (*A*) Derivative plot derived from a smoothed curve of the optical rotation ($[m']_{233}$) against temperature of S-2. Solvent is 0.1 M NaCl/20 mM phosphate, pH 7.0. Protein concentration, 1.5 mg/ml. (*B*) Amplitude of the temperature-jump signal of the S-2 melting (λ = 235 nm) is plotted as a function of temperature. Each measurement was made after a 5°C temperature jump. The absorbance changes associated with τ_f (●) and τ_s (○) reactions were then recorded at the mean of the initial and final temperatures. Both curves show maxima around 43°C, the t_m of the S-2 melting profile in *A*. S-2 sample (1.5 mg/ml) and solvent same as in *A*. (*C*) Equilibrium melting curves of S-2 (○) and rod (●) obtained at 235 nm in a spectrophotometer. S-2 and rod concentrations were 1.5 and 1.8 mg/ml, respectively. The solvent for S-2 was identical to that given in *A* and for the rod was 0.5 M NaCl/20 mM phosphate buffer, pH 7.0. Midpoints of transitions are indicated by arrows.

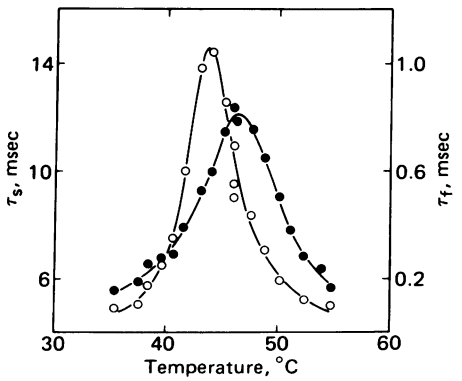

FIG. 4. Variation of the two relaxation times of S-2 melting with temperature. The two relaxations shown in Fig. 2 are plotted at the final temperature of each measurement. τ_s (○) exhibits a maximum around 43°C; τ_f (●) shows a maximum around 46°C. A 5°C temperature jump was performed; S-2 concentration was 1.5 mg/ml.

UV Absorbance Changes Accompanying Melting of Myosin Rod. The temperature-jump experiment was also performed on solutions of the myosin rod in 0.5 M NaCl at pH 7. The signal could be resolved into two relaxations similar to those shown for S-2 (Fig. 3*B*). However, the signal plotted against temperature in the rod experiment exhibits two peaks, one at 45°C and one at 52°C, in contrast to the single peak obtained for S-2. This result indicates that the rod melting is a complex process, with at least two distinct melting transitions. Burke *et al.* (15) reported earlier that the α-helical conformation of the rod melts in two steps with t_m of 44 and 55°C based on their studies of optical rotation against temperature of this particle. We find two steps with similar t_m in the A_{235} melt curve (Fig. 3*C*). The midpoint of the lower transition corresponds to that of the S-2 region when the melting curves of the rod and S-2 fragments are compared under identical solvent conditions.

The optical transition curve of myosin rod was obtained in 0.5 M NaCl; that of S-2 was taken in 0.1 M NaCl. When the S-2 melting behavior was studied as a function of NaCl concentration, it was found that the transition midpoint, t_m, increased with salt concentrations and reached 45°C at 0.5 M. This result suggests that the lower transition of rod is the melting transition of the S-2 portion of this fragment, whereas the higher transition of the rod probably reflects melting of the LMM segment of this structure.

Relaxation times of the lower temperature transition of rod are comparable to those observed in the S-2 fragment (τ_f = 0.6 msec; τ_s = 10 msec, after a temperature jump between 40° and 45°C).

DISCUSSION

The partial melting of the S-2 segment of myosin and its increased flexibility at physiological ionic strength and temperature are relevant to any mechanism in which this segment is released from the thick filament surface during a contractile cycle. The model of Huxley and Simmons (2, 3) is based primarily on their studies of mechanical transients, in which an abrupt step change in length (≈1%) was imposed on a muscle fiber in isometric contraction. For frog muscle at 4°C, four stages in the tension response are observed after a sudden reduction in length: T_1, an instantaneous tension drop; T_2, rapid recovery of tension within the next 1–2 msec; T_3, reduction or reversal of tension recovery in the next 5–20 msec; and T_4, gradual recovery of the initial isometric tension. Conversely, when the fiber is abruptly stretched, an instantaneous rise in tension is followed by rapid decay within a few msec. Again, the two early phases, T_1 and T_2, are followed by two distinctly slower stages in the tension recovery process. Since both the T_1 and T_2 responses are proportional to the amount of overlap between thick and thin filaments, the structural components responsible for these early phases are believed to reside in the crossbridges. In the early phases, T_1 and T_2, of the tension against time curves, the responses are so rapid that, on the Huxley–Simmons model, there is no attachment or detachment of crossbridges. In the later stages, T_3 and T_4, the bridges are actively cycling between attached and detached positions. In this model (see Fig. 5*A*), each crossbridge contains an instantaneous elastic element and an element in series with it that can maintain tension while taking up limited, but substantial, amounts of length change (10–12 nm). Although Huxley and Simmons have tentatively identified the S-2 segment as the elastic element and rotation of the S-2 subunit relative to the thin filament as the process responsible for the quick recovery transient, they emphasize (3) that the two structural components could be located in different regions of the crossbridge and possibly even in the thin filament.

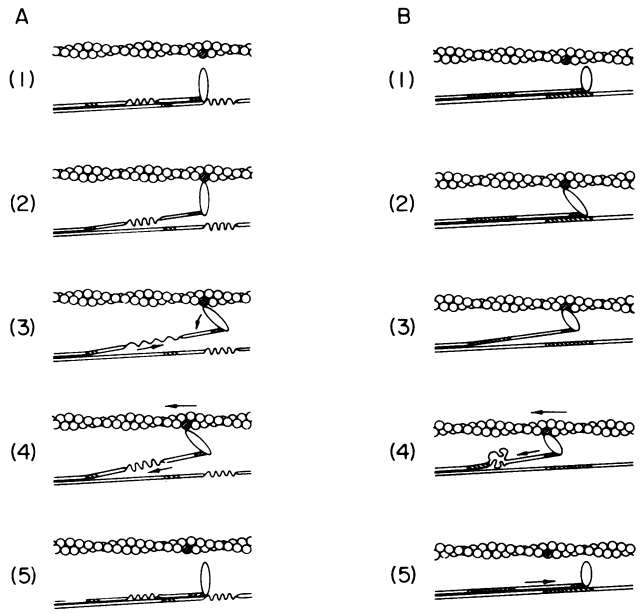

FIG. 5. (*A*) Huxley–Simmons model: 1, resting state; 2, attachment of S-1 to actin filament; 3, rotation of S-1 while it is attached to the actin filament and simultaneous stretching of the spring-like elastic component in S-2; 4, power stroke resulting from retraction of elastic component; 5, return of crossbridge to resting state. (*B*) Helix–coil model: 1, resting state; 2, S-1 swivels to attach to actin filament; 3, release of S-2 from thick filament surface; 4, power stroke resulting from helix–coil transition in S-2; 5, return of crossbridge to resting state. Long hatched region in *B* represents sticky "hinge" region of S-2 (see ref. 10).

The temperature-jump experiments on the long S-2 subfragment and myosin rod reported here indicate that the relaxation times of opening and closing the double α helix of S-2 are in the range observed for the quick recovery process observed in muscle fibers. The transient tension measurements of Huxley and Simmons have been made at 4°C on frog muscle, but a comparable rate constant (1 msec) has been found by Barden and Mason (20) in the early recovery phase following quick release of semitendinosus fibers of the toad *Bufo marinus* at 10°C. Additionally, Blangé *et al.* (21) have reported quick release experiments on rat soleus muscle at 30°C which show similar behavior. Following an instantaneous drop in tension, the quick recovery process (T_2) is completed within 0.2–0.5 msec. We would like to suggest that the two structural components responsible for T_1 and T_2 are both confined to the S-2 region of myosin. We view the initial drop in tension following an abrupt reduction in length in isometrically contracting muscle as resulting from an instantaneous decrease in the intrinsic elasticity of the partially melted S-2 structure, and the subsequent rapid tension recovery to the formation of additional coil at the expense of helix as the S-2 structure readjusts to its new decreased length (15, 22). Conversely, if the fiber is subjected to a sudden stretch, an abrupt rise in tension is expected as a result of the intrinsic elasticity of the partially melted S-2. This would be followed by a rapid decay in tension as part of the random coil region is rapidly transformed to the α-helical state to accommodate the imposed increment in length. These properties are completely consistent with the known melting–crystallization behavior of polymeric systems under an applied tensile force (23).

Our recent crosslinking experiments on glycerinated rabbit psoas myofibrils, and muscle fibers indicate that the S-1 subunit is of sufficient length (>185 Å) to span the gap between thick and thin filaments in the rigor-linkage orientation (6, 8). These

studies also reveal that a major fraction of the S-2 region of myosin remains close to the thick filament surface even under environmental conditions (pH 9, $\mu \approx 0.01$ M) where the actin-attached S-1 subunits are released from the thick filament surface and where the lattice spacing (myosin-to-actin) approximates that of a fully contracted muscle (24). This interpretation is supported by the observation that HMM (with long S-2 tail) has a marked tendency to bind to the thick filament backbone, as shown by ultracentrifuge studies of tryptic digests of synthetic myosin filaments (8, 25).

Let us now consider a model (Fig. 5*B*) in which the S-2 linkage is stabilized in the double α-helical conformation in the resting state (i.e., when this segment is part of the thick filament surface). After activation, the S-1 subunit swivels to attach to the thin filament. This process is immediately followed by release of the S-2 segment from the stabilizing environment of the thick filament surface, resulting in a rapid helix–coil transformation of a part of the folded S-2 structure. Tension is now developed within the crossbridge because the most probable distance between the ends of the resulting random coil is smaller than for the α helix. At the end of the power stroke and after release of the split products (Mg-ADP, and P_i), Mg-ATP binds to the actin-attached S-1 subunit and releases the crossbridge, allowing it to return to the stable resting state position where S-2 is bound to the thick filament surface. The force developed in such a process will be directly proportional to the number of residues undergoing the helix–coil transition and can be calculated from classical polymer theory (see equation 4 of ref. 23). The ratio of the length of the resulting coil to that of the α helix can be approximated by the relation, $L_{RC}/L_{\alpha} = 7.6/\sqrt{n}$, in which n is the number of residues in the α-helical state (26). Assuming that the power stroke ends when the tension approaches zero, melting of 150–170 residues per strand would contract the S-2 structure along its axis (it is fixed at the LMM/HMM and S-1/S-2 junctions) by about 10–12 nm.

Mason (22) has recently determined the ratio of stiffness to tension in an activated frog sartorius muscle fiber vibrating sinusoidally at 300 Hz. This ratio remains constant over a 50-fold change in tension, suggesting, in agreement with Huxley and Simmons, that the crossbridges are the source of tension and dynamic stiffness. The magnitude of stiffness/tension ratio is consistent with a partially helical-partially coiled structure within each crossbridge and can be explained by a helix–coil transition of about 80 residues in each strand of the S-2 structure at limiting values of the vibration frequency.

We thank Dr. Peter Knight for very helpful discussions. This research was supported by National Institutes of Health Grant AM-04349 to W.F.H. and National Science Foundation Grant PCM-75-08690 to T.Y.T.

1. Huxley, H. E. (1969) *Science* **164,** 1356–1366.
2. Huxley, A. F. & Simmons, R. M. (1971) *Nature (London)* **233,** 533–538.
3. Huxley, A. F. & Simons, R. M. (1972) *Cold Spring Harbor Symp. Quant. Biol.* **37,** 669–680.
4. Podolsky, R. J. & Nolan, A. C. (1972) *Cold Spring Harbor Symp. Quant. Biol.* **37,** 661–668.
5. Harrington, W. F. (1971) *Proc. Natl. Acad. Sci. USA* **68,** 685–689.
6. Sutoh, K. & Harrington, W. F. (1977) *Biochemistry* **16,** 2441–2449.
7. Sutoh, K., Chen-Chiao, Y.-C. & Harrington, W. F. (1978) *Biochemistry* **17,** 1234–1239.
8. Chen-Chiao, Y.-C. & Harrington, W. F. (1979) *Biochemistry,* in press.
9. Weeds, A. G. & Pope, B. (1977) *J. Mol. Biol.* **111,** 129–157.
10. Sutoh, K., Sutoh, K., Karr, T. & Harrington, W. F. (1978) *J. Mol. Biol.* **126,** 1–22.
11. Weeds, A. G. & Taylor, R. S. (1975) *Nature (London)* **257,** 54–56.
12. Harrington, W. F. & Burke, M. (1972) *Biochemistry* **11,** 1448–1455.
13. Eigen, M. & De Maeyer, L. C. (1963) in *Techniques of Organic Chemistry,* eds. Freiss, S. L., Lewis, E. S. & Weissberger, A. (Interscience-Wiley, New York), Vol. 8, Part 2, pp. 845–1054.
14. Tsong, T. Y., Tsong, T. T., Kingsley, E. & Siliciano, R. (1976) *Biophys. J.* **16,** 1091–1104.
15. Burke, M., Himmelfarb, S. & Harrington, W. F. (1973) *Biochemistry* **12,** 701–710.
16. Lowey, S., Slayter, H. S., Weeds, A. G. & Baker, H. (1969) *J. Mol. Biol.* **42,** 1–29.
17. Schwartz, G. & Seelig, J. (1968) *Biopolymers* **6,** 1263–1277.
18. Baldwin, R. L. (1975) *Annu. Rev. Biochem.* **44,** 453–475.
19. Kanehisa, M. I. & Tsong, T. Y. (1978) *J. Mol. Biol.* **124,** 177–194.
20. Barden, J. A. & Mason, P. (1978) *Science* **199,** 1212–1213.
21. Blangé, T., Karemaker, J. M. & Kramer, A. E. J. L. (1972) *Pflügers Arch.* **336,** 277–288.
22. Mason, P. (1978) *Biophys. Struc. Mechanism* **4,** 15–25.
23. Flory, P. J. (1956) *Science* **124,** 53–60.
24. Rome, E. (1968) *J. Mol. Biol.* **37,** 331–334.
25. Harrington, W. F., Sutoh, K. & Chen-Chiao, Y.-C. (1978) in *John Marshall Symposium on Motility in Cell Function,* ed. Pepe, F. (Academic, New York), in press.
26. Flory, P. J. (1969) *Statistical Mechanics of Chain Molecules.* (Interscience-Wiley, New York), pp. 30–47.